ELSEVIER

Journal of Power Sources 63 (1996) 41–45

JOURNAL OF POWER SOURCES

In situ X-ray diffraction studies of a graphite-based Li-ion battery negative electrode

A.H. Whitehead [a,*], K. Edström [b], N. Rao [c], J.R. Owen [a]

[a] *Department of Chemistry, University of Southampton, Southampton SO17 1BJ, UK*
[b] *Institute of Chemistry, University of Uppsala, Box 531, 751 21 Uppsala, Sweden*
[c] *Danionics A/S, Hestehaven 21 j, 5260 Odense S, Denmark*

Received 12 March 1996; revised 11 June 1996; accepted 2 July 1996

Abstract

Lithium–graphite intercalation compounds were synthesised in an electrochemical cell by the application of a series of current pulses, during which non-equilibrium distributions of intercalation phases were created in the graphite. The phase formation and subsequent interconversion were studied by a combination of chronopotentiometry and in situ X-ray diffraction.

Keywords: Lithium; Graphite; Intercalation; Phase; X-ray diffraction

1. Introduction

Many types of carbon have been considered for use as the negative electrode materials for lithium-ion batteries [1,2]. Graphite is a promising material [3–6] as it has a low working voltage (<300 mV versus Li/Li^+), high theoretical insertion capacity — up to LiC_6 (372 mAh g^{-1}) — and is expected to lose little charge, unlike lithium metal, in film-forming and other parasitic reactions after the first charge/discharge cycle.

In contrast to many types of carbon, in which phase separation upon lithium intercalation is poorly resolved or non-existent, graphite forms several phases which can be identified in the electrochemical titration as well as by X-ray diffraction (XRD). Thus, in the lithium–graphite system, the kinetics of phase formation, as well as ionic diffusion, may determine the maximum theoretical rate at which electrodes may be cycled. Lithium intercalation under non-equilibrium conditions was studied in an effort to measure the rate of phase interconversion.

Lithium ions can insert between the carbon layers in graphite, causing the stacking pattern to change from ABAB in AAAA [7–9] with a consequent increase in the average layer spacing [10–12]. The average graphite layer spacing, which may be determined by XRD, has characteristic values for the intercalation phases. XRD has been used in quantitative determination of the different lithium–graphite intercalation compounds (Li–GICs) present in an electrode [13]. Several studies have utilised XRD to examine the equilibrium staging of electrochemically intercalated lithium in graphite [14]. It has been found that, at low insertion rates, lithium preferentially intercalates in the order: stage 1′ → stage 4 → stage 3 → stage 2L → stage 2 → stage 1 [15]. Stage 1′ is defined as a Li–GIC with stage order greater than 4 (Li_xC_6, $x<0.16$); however, it has been proposed that a stage 8 phase may exist [16]. Stage 2L corresponds to a liquid-like stage 2 phase [17] with a lower in-plane concentration of lithium than stage 2: $Li_{0.667}C_{12}$ and LiC_{12}, respectively.

2. Experimental

A paste was formed by mixing Lonza KS44-PI graphite (G.S. Inorganic Products) and carbon black (Degussa) in an ethylene/propylene copolymer (EPM, Exxon) in cyclohexane solution. The paste was spread upon 15 μm thick copper foil and the cyclohexane was allowed to evaporate. The resulting material was cut into strips and the graphite paste scraped away to define an active electrode area of approximately 0.3 cm^2. The graphite loading of the dried electrodes was 20 mg cm^{-2}.

A 1 M solution of lithium hexafluoroarsenate in a 1:1 (by mass) solution of ethylene carbonate (EC) and diethyl carbonate (DEC) was prepared in an argon filled dry box (<2 ppm water and oxygen). The DEC was decanted from 4 Å

* Corresponding author.

PII S0378-7753(96)02440-8

molecular sieves (Stavar). The lithium hexafluoroarsenate and EC were dried under vacuum prior to use.

Cells were constructed by vacuum-sealing a graphite powder electrode, a glass filter paper, soaked in the hexafluoroarsenate solution, and a lithium counter electrode into an aluminium-polymer laminate (Lamofoil™) pouch. The two electrodes were connected to nickel foils which were sealed through the edges of the bag to allow external electrical contact. Open-circuit potentials of the uncycled cells were greater than 2.75 V.

Electrochemical measurements were made by using a MacPile II™ cycling system. Concurrent XRD measurements (Cu Kα radiation) were made with a STOE powder diffractometer using a position sensitive detector (covering 7° in 2θ). The test cell was held in a purpose-built holder which rotated the sample repeatedly between two positions separated by 140° at a rate of ~3° s^{-1}. The sample was rotated to reduce the effect of preferred orientation in the graphite and polymer laminate bag. Stack pressure was applied by clamping the cell between thin beryllium sheets in the sample holder.

3. Results and discussion

3.1. Calibration

Lithium was intercalated galvanostatically into a graphite electrode, by pulsed coulometric titration (Fig. 1) at an overall rate of $C/19$ (i.e., a total time, including insertion and relaxation periods, of 19 h would be required to form LiC_6 at 100% efficiency). A series of 300 s current pulses, followed by 750 s relaxations, was applied to the cell. The end-points of individual relaxations (upper trace) were free of iR drop and were near to the equilibrium potential of the graphite electrode with respect to Li/Li^+.

XRD measurements were made during the intercalation (Fig. 2).

The XRD patterns (Fig. 2) are denoted with a letter according to the extent of titration (Fig. 1) at which they were recorded. The dominant peaks in Fig. 2 have been assigned as [18,19]:

(a) the 002 peak of graphite;

(b) two peaks: the 004 peak of the stage 4 phase and a peak corresponding to the average graphite layer spacing of Li_xC_6, $x<0.16$ (stage 1′);

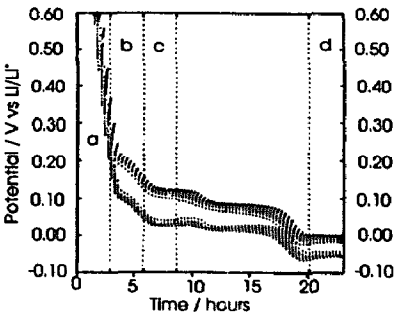

Fig. 1. Pulsed coulometric titration of lithium versus graphite powder electrode. The upper and lower curves correspond to the insertion and relaxation periods, respectively. The amount of charge passed corresponds to: (a) 0–56 mAh g^{-1}; (b) 56–113 mAh g^{-1}; (c) 113–169 mAh g^{-1}, and (d) 394–450 mAh g^{-1}.

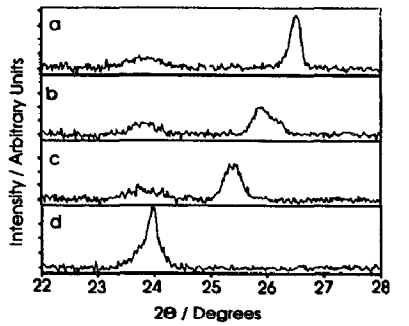

Fig. 2. X-ray diffractograms showing the (002) peak of graphite at various degrees of insertion. The amount of charge passed corresponds to: (a) 0–56 mAh g^{-1}; (b) 56–113 mAh g^{-1}; (c) 113–169 mAh g^{-1}, and (d) 394–450 mAh g^{-1}.

(c) two overlapping peaks: the 002 peaks of LiC_{12} (stage 2) and $Li_{0.667}C_{12}$ (stage 2L), and

(d) the 001 peak of LiC_6 (stage 1).

The broad peak at 23.7° has been assigned to components of the aluminium–polymer laminate bag.

The peaks in Fig. 2(a)–(d) were analysed by baseline subtraction, followed by integration between limits (method 1) and by fitting curves (Pearson VII functions) using STOE software (method 2). The peaks were normalised to the pristine graphite peak (Fig. 2(a)). The results are shown in Table 1.

The intensity of the dominant peak (Fig. 2(a)–(d)) is affected by the change in composition of the GIC and the change in scattering angle, as well as any long-term variations in the primary beam intensity. However, these effects appear to cancel out as the area of this peak (Table 1) remained

Table 1
Summary of the XRD data

Region	Layer spacing (Å)	Dominant stage [20,21]	Method 1, normalised area	Method 2, normalised area
a	3.359	pristine graphite	1.00	1.00
b	3.44, 3.39	4 and 1′	0.99	1.03
c	3.513	2 and 2L	1.01	1.05
d	3.712	1	0.98	0.99

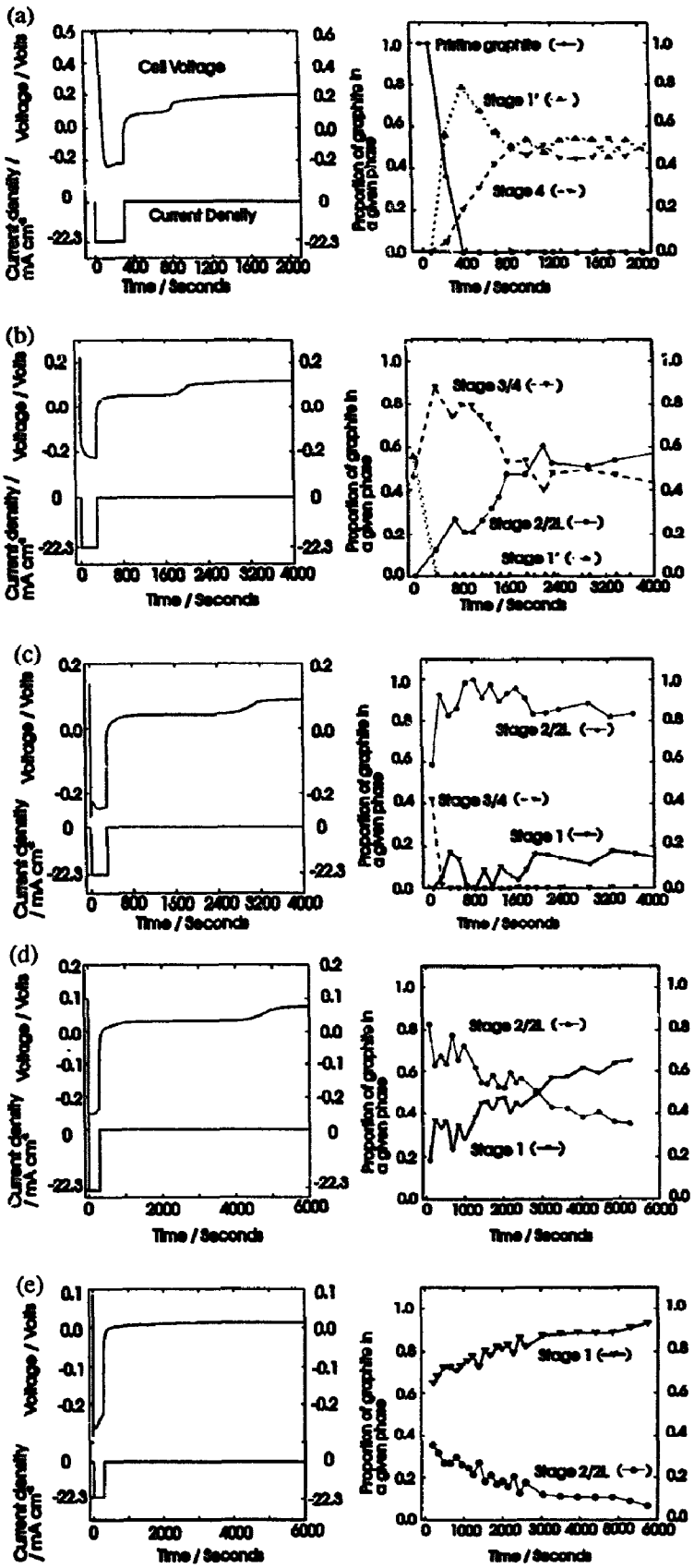

Fig. 3. Potentiometric data and corresponding phase fractions for lithium intercalated graphite, after five equal current pulses: (a)–(e), respectively.

Table 2
Summary of the measurements shown in Fig. 3

Pulse number	Charge passed (mAh g^{-1})	Voltage relaxation time (s)	Voltage at 6000 (s mV^{-1})
1	93	500	216
2	186	1700	124
3	279	2600	93
4	372	4500	77
5	465	>6000	12

constant with GIC composition within the accuracy of the above methods (± 0.04).

It was found, in accordance with the theory [22] and transient K–GIC measurements [23], that there was little broadening of the graphite peaks during the following measurements; hence, it will be assumed that the proportion of graphite present in a given phase can be deduced using Eq. (1)

$$\text{proportion of stages } x = \frac{\text{(area under peak corresponding to stage } x)}{\sum_{i=\text{all stages}} \text{(area under peak corresponding to stage } i)} \quad (1)$$

3.2. Transient measurements

A series of current pulses was passed through a test cell. The pulses were each of 300 s duration and conveyed 93 mAh g^{-1} of charge (3C charge rate). Following each pulse the cell was allowed to relax for at least 8 h (until the rate of change of cell voltage was below 2 mV h^{-1}). In situ XRD data were recorded every 150 s from the start of the current pulse ($t=0$) for 2400 s, after which diffractograms were recorded every 450 s. The XRD data were analysed as above (Eq. (1)).

The proportion of a given phase is accurate to ± 0.05, except that of stage 1, which is accurate to ± 0.10.

The amount of pristine graphite was found to become negligible (<5 mol%) within 400 s of the start of the initial current pulse (Fig. 3(a)). Thus, in excess of 95% of the electrode was accessible to lithium intercalation.

Following the first current pulse stage 1′ Li–GIC was formed, which was then converted to stage 4 phase. The growth of the stage 4 phase became negligible 500 s after the end of the current pulse. Similarly, it can be seen (Fig. 3(a)–(e)) that phase interconversion continued during each relaxation period subsequent to each current pulse. The rate of phase interconversion decreased with charge passed until, after the final pulse (Fig. 3(e)), phase interconversion continued for 5000 s. One apparent exception is the phase interconversion after the third pulse; however, it was not possible, from the XRD data, to distinguish stage 2 from stage 2L. Hence, it may be expected that some undetected phase interconversion was proceeding, even though the sum of proportions of the two stage 2 phases remained virtually unchanged after 2000 s.

It can be seen (Fig. 3(a)–(d)) that, during the first four current relaxations ($t>300$ s), the cell voltage passes through a final point of inflection. This reflects a sharp decrease in surface activity of the graphite electrode. The time at which the inflection occurred, after the current pulse, (voltage relaxation time) was found to increase as the degree of lithium intercalation increased (Table 2), however, it should be noted that the faradaic yield of LiC_6 was approximately 80% (Fig. 3(e)).

The initial relaxation voltage plateau lies at a more negative potential than the final one, indicative of high-activity phases or the presence of metallic lithium at the graphite surface. The two voltage plateaus recorded after the third pulse (Fig. 3(c)) were indicative of phase interconversions, which were not apparent from the XRD data, as mentioned above. However, after the fifth pulse, the XRD data reveals phase interconversions even though there was only a single voltage plateau. From these observations it is clear that chronopotentiometry and XRD are complementary techniques in the evaluation of phase interconversion in the Li–GIC system.

The presence of a minority concentrated phase, after the first current pulse, may be inferred from the XRD peak positions (Fig. 4). Layer spacings, calculated for the dominant XRD peaks, of >3.45 Å were found at short times ($t<600$ s). These spacings are indicative of a mixture of stage 3 and stage 4 Li–GICs, but stage 1′ was also present (lower trace). Thus, a mixture of at least three phases existed in the electrode [24]. At longer times, the layer spacing of the more concentrated phases (upper trace) decreased, implying a decrease in the ratio of stage 3 to stage 4.

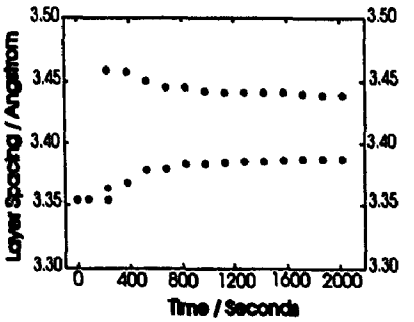

Fig. 4. Layer spacings for the dominant XRD peaks after the first current pulse.

Fig. 5. Schematic representation of lithium activity in a graphite particle during intercalation. Depth of shading indicates lithium activity.

Following the third, fourth and fifth pulses, the two dominant peaks, corresponding to stage 1 and stage 2 (or stage 2L), are found to vary little in position: 3.700 ± 0.015 and 3.515 ± 0.005 Å, respectively. It may also be noted that no intermediate phases, e.g. stage 1.5, were detected, even at short times. However, after the third pulse, the initial relaxation plateaus may indicate plated lithium rather than concentrated Li–GIC phases. This is almost certainly the case after the fifth pulse, where the voltage remained below 20 mV for more than 21 h [25].

In the long-time limit (2–10 h), after the first four pulses, the proportion of phases present and the cell voltage remained constant. In this limit, activity may be expected to differ little between the bulk and surface of the graphite particles (Fig. 5).

4. Conclusions

It has been shown that in situ XRD and chronopotentiometry are complementary and of great value in elucidating the structural changes that occur during intercalation. Chronopotentiometry generally revealed the presence of two voltage plateaus during the relaxation of the unsaturated electrode after current pulses, but only one when metallic lithium was plated onto a saturated electrode.

The following model has been proposed, for the two plateau situations.

1. The initial plateau corresponds to a dynamic system in which concentrated lithium phases are present at the surface of the graphite particles. From these phases, lithium diffuses to the more dilute bulk phases. As this happens, the ratio of high to low stage order Li–GICs increases.
2. The second voltage plateau extends for more than 10 h after each pulse. In this region, the Li–GICs remain in an almost constant ratio, indicating that the reservoir of lithium ions in concentrated surface phases has become depleted to an insignificant level.

The transition between the two plateaus occurred at longer time periods as the total lithium concentration of the electrode increases. To optimise charging efficiency lithium plating should be avoided; thus, an optimal electrode charging regime may apply an insertion current that decreases as the lithium concentration of the electrode increases.

It may also be concluded that lithium intercalates into the graphite particles from plated metallic deposits, although the mechanism for this process is unclear.

Acknowledgements

This work was supported financially by the E.C. Joule II programme and, in part, by the Swedish Natural Science Council (NFR) and NUTEK in Sweden. The authors would like to thank Professor Josh Thomas (University of Uppsala) for initiating the collaboration and for his many helpful suggestions.

References

[1] D. Fauteaux and R. Koksbang, *J. Appl. Electrochem., 23* (1993) 1.
[2] K.M. Abraham, *Electrochim. Acta, 38* (1993) 1233.
[3] M. Arakawa and J.-I. Yamaki, *J. Electroanal. Chem., 219* (1987) 273.
[4] K. Sawai, Y. Iwakoshi and T. Ohzuku, *Solid State Ionics, 69* (1994) 273.
[5] J.R. Dahn, A.K. Sleigh, H. Shi, J.N. Reimers, Q. Zhong and B.M. Way, *Electrochim. Acta, 38* (1993) 1179.
[6] Y. Takasu, H. Shiinoki and Y. Matsuda, *J. Electrochem. Soc., 131* (1984) 959.
[7] D. Guérard and A. Hérold, *Carbon, 13* (1975) 337.
[8] J. Rossat-Mignod, A. Wiedenmann, K.C. Woo, J.W. Milliken and J.E. Fischer, *Solid State Commun., 44* (1982) 1339.
[9] S. Rabii, J. Chomilier and G. Loupias, *Phys. Rev. B, 40* (1989) 10105.
[10] J.C. Charlier, X. Gonze and J.P. Michenaud, *Carbon, 32* (1994) 289.
[11] C.R. Houska and B.E. Warren, *J. Appl. Phys., 25* (1954) 1503.
[12] R. Juza and V. Wehle, *Naturwissenschaften, 52* (1965) 560.
[13] J.R. Dahn, R. Fong and M.J. Spoon, *Phys. Rev. B, 42* (1990) 6424.
[14] D. Aurbach and Y. Ein-Eli, *J. Electrochem. Soc., 142* (1995) 1746.
[15] D. Billaud, F.X. Henry and P. Willmann, *Mater. Res. Bull., 28* (1993) 477.
[16] T. Ohzuku, Y. Iwakoshi and K. Sawai, *J. Electrochem. Soc., 140* (1993) 2490.
[17] M. Inaba, H. Yoshida, Z. Ogumi, T. Abe, Y. Mizutami and M. Asano, *J. Electrochem. Soc., 142* (1995) 20.
[18] J.R. Dahn, *Phys. Rev. B, 44* (1991) 9170.
[19] D. Billaud, F.X. Henry and P. Willmann, *Mol. Cryst. Liq. Cryst., 245* (1994) 159.
[20] Z. Jiang, M. Alamgir and K.M. Abraham, *J. Electrochem. Soc., 142* (1995) 333.
[21] N. Takami, A. Satoh, M. Hara and T. Ohsaki, *J. Electrochem. Soc., 142* (1995) 371.
[22] H. Miyazaki and C. Horie, *Synth. Met., 12* (1985) 149.
[23] R. Nishitani, Y. Uno and H. Suematsu, *Phys. Rev. B, 27* (1983) 6572.
[24] G. Kirczenow, *Can. J. Phys., 66* (1988) 39.
[25] R. Yazami and Ph. Touzain, *J. Power Sources, 9* (1983) 365.